ADVANCED OPTICAL MATERIALS
www.advopticalmat.de

Frequency-Agile Temporal Terahertz Metamaterials

*Prakash Pitchappa, Abhishek Kumar, Haidong Liang, Saurav Prakash, Nan Wang, Andrew A. Bettiol, Thirumalai Venkatesan, Chengkuo Lee, and Ranjan Singh**

Spatiotemporal manipulation of electromagnetic waves has recently enabled a plethora of exotic optical functionalities, such as non-reciprocity, dynamic wavefront control, unidirectional transmission, linear frequency conversion, and electromagnetic Doppler cloak. Here, an additional dimension is introduced for advanced manipulation of terahertz waves in the space-time, and frequency domains through integration of spatially reconfigurable microelectromechanical systems and photoresponsive material into metamaterials. A large and continuous frequency agility is achieved through movable microcantilevers. The ultrafast resonance modulation occurs upon photoexcitation of ion-irradiated silicon substrate that hosts the microcantilever metamaterial. The fabricated metamaterial switches in 400 ps and provides large spectral tunability of 250 GHz with 100% resonance modulation at each frequency. The integration of perfectly complementing technologies of microelectromechanical systems, femtosecond optical control and ion-irradiated silicon provides unprecedented concurrent control over space, time, and frequency response of metamaterial for designing frequency-agile spatiotemporal modulators, active beamforming, and low-power frequency converters for the next generation terahertz wireless communications.

Terahertz waves lie in between the electronics (microwaves) and photonics (infrared) realms of the electromagnetic spectrum and hence combines the advantages of both spectral regions. Terahertz waves provide high frequency field oscillations, low photon energy, high directionality, and high transparency through most material systems. These unique properties of terahertz waves have been exploited for both fundamental sciences and advanced applications, alike. However, these properties have also been a bane and has significantly hindered the development of efficient terahertz technologies. However, in recent years, research effort in terahertz technologies has been accelerated from both electronics as well as photonics communities, owing to its immense potential, especially in high-speed wireless communication, non-destructive imaging, high resolution spectroscopy, and for probing of ultrafast field driven as well as ultrastrong energy coupled processes.[1–8] One of the major challenges in the manipulation of terahertz waves is its minimal interaction with naturally occurring materials. Hence, cavity based resonant terahertz interaction has been widely explored using metamaterials.[9–12] Metamaterials are artificially patterned sub-wavelength structures, whose optical properties are predominantly determined by the pattern geometry. Hence, metamaterials are topographically flat, functionally versatile, and highly scalable. Furthermore, integration of dynamic materials or structurally reconfigurable microstructures within metamaterial resonators allow for on-demand

Dr. P. Pitchappa, A. Kumar, Prof. R. Singh
Division of Physics and Applied Physics
School of Physical and Mathematical Sciences
Nanyang Technological University
21 Nanyang Link, Singapore 637371, Singapore
E-mail: ranjans@ntu.edu.sg

Dr. P. Pitchappa, A. Kumar, Prof. R. Singh
Centre for Disruptive Photonic Technologies
The Photonic Institute
50 Nanyang Avenue, Singapore 639798, Singapore

Dr. P. Pitchappa, Dr. N. Wang
Institute of Microelectronics
Agency for Science, Technology and Research (A*STAR)
2 Fusionopolis Way, Singapore 138634, Singapore

Dr. H. Liang, S. Prakash, Prof. T. Venkatesan
NUSNNI-NanoCore
National University of Singapore
Singapore 117411, Singapore

The ORCID identification number(s) for the author(s) of this article can be found under https://doi.org/10.1002/adom.202000101.

DOI: 10.1002/adom.202000101

Dr. H. Liang, Prof. A. A. Bettiol
Centre for Ion Beam Applications (CIBA)
Department of Physics
National University of Singapore
Singapore 117542, Singapore

S. Prakash, Prof. T. Venkatesan
NUS Graduate School for Integrative Science and Engineering
National University of Singapore
Singapore 117456, Singapore

Prof. A. A. Bettiol, Prof. T. Venkatesan
Department of Physics
National University of Singapore
Singapore 117542, Singapore

Prof. T. Venkatesan, Prof. C. Lee
Department of Electrical and Computer Engineering
National University of Singapore
Singapore 117583, Singapore

Prof. T. Venkatesan
Department of Materials Science and Engineering
National University of Singapore
Singapore 117575, Singapore

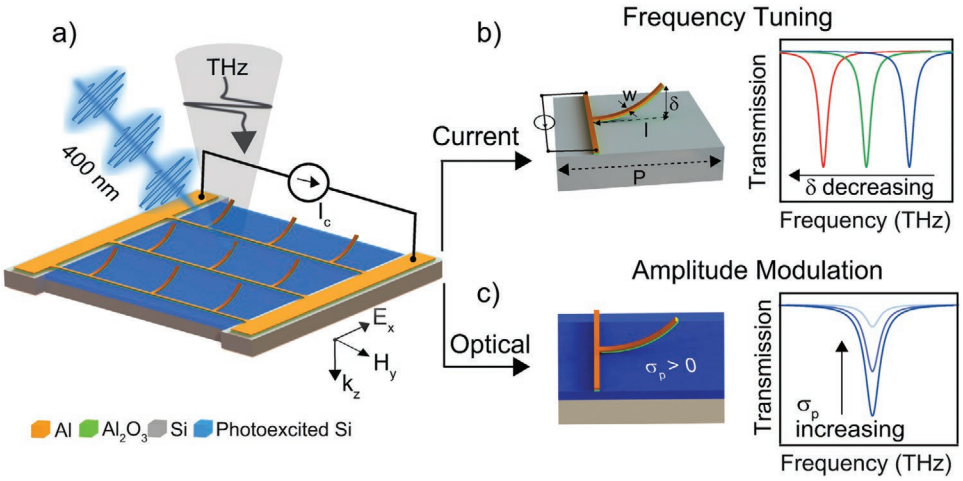

Figure 1. a) Schematic representation of the microcantilever metamaterial. The unit cell is the out-of-plane deformable bimorph microcantilever. The dimensions of the microcantilever unit cell are as follows (cf. the schematic in (b)): periodicity (P) = 120 µm, length (l) = 60 µm, width (w) = 5 µm, microcantilever tip displacement (δ). The thickness of Al and Al_2O_3 is 300 and 50 nm, respectively. b) Resonance frequency tunability with current stimulus. With increasing current, the temperature increases and causes the bimaterial microcantilever to bend down towards the substrate (δ decreasing), thereby leading to a redshift in the resonance frequency. c) Resonance modulation under optical stimulus. At given resonance frequency, when 400 nm is incident on ion-irradiated Si, the photoconductivity of Si (σ_p) increases thereby leading to the modulation of resonance strength.

control of terahertz waves and are popularly termed as "reconfigurable metamaterials".[13–15] Reconfigurable metamaterials have been reported for active control of various aspects of terahertz waves, such as amplitude modulation,[16–18] frequency agility,[19–23] polarization switching,[24–26] phase manipulation,[27,28] and frequency conversion.[29] However, these reports are currently limited to control of a single dynamical parameter. Manipulation of terahertz waves across varied dimensions of space, time and frequency will enable advanced and efficient terahertz devices for real world applications.

One of the widely studied terahertz reconfigurable metamaterials is the ultrafast terahertz resonance modulator, owing to its importance in next generation high speed wireless communication systems.[30] Ultrafast modulators with picosecond switching speeds have been realized through femtosecond optical pulse control of metamaterials integrated with a variety of photoresponsive materials, including conventional semiconductors,[16,31,32] perovskites,[33–35] 2D materials,[36–39] phase-change materials,[40,41] and superconductors.[42,43] However, these demonstrations are limited to narrowband operation, owing to the inherent resonant nature of metamaterials. This limitation can be overcome by expanding the control to the spectral domain that allows for the tuning of resonance frequency and hence a larger operational bandwidth.

Here, we report a microcantilever metamaterial integrated on an ion-irradiated silicon (Si) substrate as shown in **Figure 1**a, to achieve desired terahertz resonance frequency and amplitude, as schematically shown in Figures 1b and 1c, respectively. The multidomain manipulation of terahertz waves is realized through the integration of two complementing approaches—microelectromechanical systems (MEMS) that provide large spectral tunability and optical control using femtosecond laser pulses that provide ultrafast amplitude modulation. Released bimaterial microcantilever is used as the cut wire resonator (CWR) metamaterial unit cell. The spectral control is realized through Joule heating with input electrical current, which causes the bimaterial microcantilevers to deform in the out-of-plane direction. This deformation then leads to a continuously tunable dipolar resonance frequency of the CWR metamaterial, as schematically shown in Figure 1b. The ultrafast temporal response on the other hand is achieved through photoexcitation of Si substrate with 3.1 eV optical pump. Upon optical pumping, photoexcited carriers on Si surface screen the confined terahertz field, thereby leading to a resonance amplitude modulation, as schematically shown in Figure 1c. The charge carrier relaxation time of single crystal Si substrate was significantly enhanced through ion-irradiation technique and resonance switching time of ≈400 ps was experimentally achieved. The proposed hybrid approach allows for the expanded operation of the current narrowband modulators over a wider bandwidth. Furthermore, the additional electrical control can be further exploited for spatially resolved control.[20] This can potentially enable complete control of terahertz waves across spatial, spectral, polarization, and temporal domains. Generically, multidomain manipulation of electromagnetic waves is critical for the realization of spatiotemporal metamaterials, frequency-agile time varying metamaterials, colour tunable ultrafast modulators, and various other novel devices.[44,45] Hence, the strategy of employing multiple independent stimulus not only enhances the functionality of existing single stimulus approach but will also aid in the demonstration of novel exotic phenomena.

The proposed reconfigurable metamaterial consists of a 2D array of CWRs with square periodicity of P = 120 µm as shown in Figure 1a. The length of the CWR, l = 60 µm, and width, w = 5 µm, respectively as shown in Figure 1b. The CWR is made of bimaterial layer consisting of 300 nm aluminum (Al) on top of 50 nm aluminum oxide (Al_2O_3). The microcantilever metamaterial is fabricated on a lightly doped Si substrate using a CMOS compatible process (see Experimental Section). After release, the microcantilevers are deformed upwards owing to the residual stress between the Al and Al_2O_3 layers, as shown in Figure 1a. In order to achieve active reconfiguration of the microcantilevers,

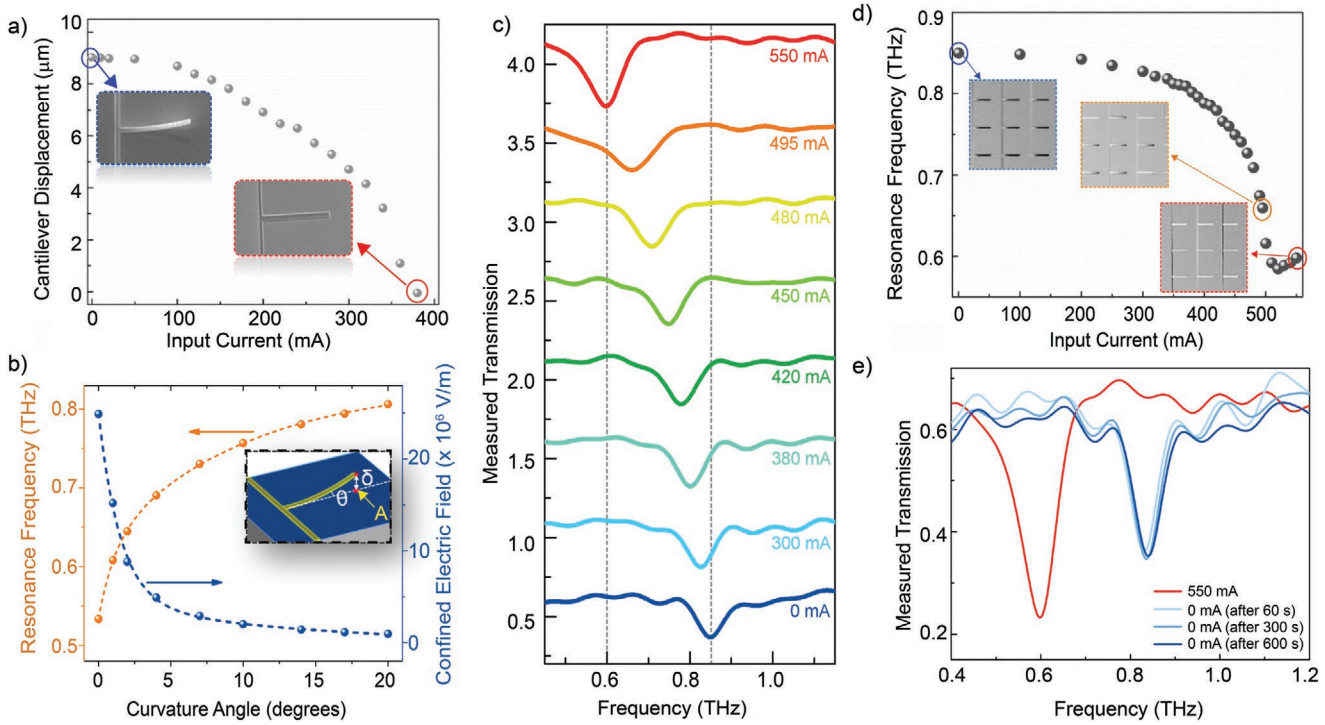

Figure 2. a) Measured microcantilever tip displacement (δ) with increasing current. The insets show the scanning electron microscope (SEM) image of the microcantilever at 0 and 380 mA, respectively. b) Simulated microcantilever metamaterial resonance frequency (orange) and the field confined at "A" on the Si surface under the microcantilever tip for increasing tip displacement. The dotted line represents the single exponential fit. c) Measured transmission spectra of the microcantilever metamaterial with increasing input current. d) Measured resonance frequency with increasing input current with the inset showing the optical image of the microcantilever metamaterial signifying its state at 0, 495, and 550 mA. e) Measured transmission spectra of the microcantilever metamaterial at different time intervals (60, 300, and 600 s) after switching off from 550 mA.

electrothermal actuation mechanism was employed by applying current across the entire metamaterial. When current is applied across the Al lines, Joule's heating increases the temperature of the entire metamaterial. With increasing temperature, Al expands much more than Al_2O_3 and since Al is placed on top of Al_2O_3, the bimaterial microcantilevers deform downward, that is, towards the substrate.[21] The out-of-plane deformation of the microcantilever at any given input current primarily depends on the microcantilever geometry, differential thermal expansion coefficient of the constituent materials and the heat loss pathways. The mechanical profile of the released microcantilever under varying input current was characterized using a digital holographic microscope (Figure S1, Supporting Information). The out-of-plane tip displacement of microcantilever (δ) with respect to input current is shown in **Figure 2**a. The tip displacement (δ) after release is measured to be ≈9 μm. With increasing current, the microcantilevers deform continuously as expected. Maximum deformation is achieved at 380 mA, when the microcantilever comes in physical contact with the Si substrate (i.e., $\delta = 0$ μm). Hence, the overall actuation range of the microcantilever is primarily limited by the initial displacement of the microcantilever. This initial displacement can be readily engineered through varying combination of bimaterial layers, their relative thicknesses and cantilever release geometry.[46,47] Here, we chose Al and Al_2O_3 as the bimaterial layers, owing to their CMOS compatibility, large difference in thermal expansion coefficient and robustness to vapor hydrofluoric acid release.

To elucidate the terahertz response of the microcantilever metamaterial, simulations were carried out using frequency domain solver in computer simulation technology (CST) software. The deformed microcantilever was modelled by bending the straight microcantilever with specific curvature angle to achieve desired tip displacement (see Figure S2a, Supporting Information). The incoming terahertz wave impinged at normal incidence with electric field along the length of the microcantilever. The transmission spectrum of the microcantilever metamaterial was simulated with increasing tip displacement (see Figure S2b, Supporting Information). The simulated CWR resonance frequency with respect to tip displacement is shown in Figure 2b. When $\theta = 20°$, the resonance frequency is at 0.8 THz. At this frequency, the surface current is along the length of the microcantilever and in-phase with the incident electric field of the terahertz wave, which indicates the excitation of electric dipole resonance (see Figure S2d, Supporting Information). With decreasing θ, redshift in the resonance frequency is observed. This is due to the increase in effective out-of-plane capacitance that is formed between the Al layer of the microcantilever and Si substrate.[33,46] At $\theta = 0°$, the resonance frequency is at 0.53 THz. The simulated surface current is in-phase with the electric field of the incident terahertz waves (see Figure S2e, Supporting Information), confirming the electrical dipole nature of the resonance. The resonance frequency tunability from the simulated spectra was calculated for each curvature angle "θ" as $\Delta f/f_{20} = (f_{20} - f_\theta)/f_{20}$ where f_{20} is the resonance

frequency of the microcantilever metamaterial at $\theta = 20$, which corresponds to the fabricated metamaterial without any input current. (See Figure S2c, Supporting Information). Simulated tunable range (Δf) of the dipolar resonance frequency of the microcantilever metamaterial was 0.27 THz and maximum tunability ($\Delta f/f_{20}$) of ≈35% was achieved. Hence, the change in resonance frequency for a given tip displacement difference is more significant when the microcantilever is closer to the substrate than when it is further away.[48] Furthermore, the confined field at the top surface of Si substrate directly below the cantilever tip was determined from the simulation results as shown in Figure 2b. The field on top surface of Si substrate decreases with increasing θ, which also confirms the reduction in confined field strength.

The spectral tunability of the fabricated microcantilever metamaterial was characterized using a terahertz time domain spectroscopy system (see Experimental Section). Figure 2c shows the measured transmission spectra of the metamaterial at varying input current. The resonance frequency of the metamaterial at 0 mA was measured to be 0.85 THz and it continuously red-shifted with increasing current. At 550 mA, the maximum deformation was achieved, and the resonance frequency of the metamaterial was measured to be at 0.6 THz. A continuously tunable range of 0.25 THz was experimentally achieved. Measured resonance frequency tunability was calculated as $\Delta f/f_0$, where Δf is the change in resonance frequency for a given input current and f_0 is the resonance frequency of the metamaterial at 0 mA input current (see inset of Figure S2c, Supporting Information). The maximum tunability of ≈30% was achieved for the input current of 550 mA. A resonance broadening effect was observed for the input current of 495 mA, which comes from the non-homogeneity of the fabricated microcantilevers forming the metamaterial as shown in the inset of Figure 2d. The effect of non-homogeneity is more pronounced when the cantilevers are closer to the substrate, owing to strong change in the confined fields. The measured resonance frequency of the metamaterial with increasing current is shown in Figure 2d and the trend matches well with the simulated results as shown in Figure 2b (orange line). The minor discrepancy between the simulated and measured values of resonance frequency could be caused due to fabrication errors and mismatch in properties of the constituent materials. Optical images of the fabricated microcantilever metamaterial with increasing current clearly shows that all the microcantilevers forming the metamaterial move downwards (see Figure S3, Supporting Information). However, a discrepancy is observed in the value of critical current required to switch the microcantilever in the deformation study (I_c = 380 mA), optical imaging (I_c = 420 mA), and terahertz transmission measurement (I_c = 550 mA). This is caused due to the difference in the conduction and convection heat losses in these experimental setups. It is important to note that electrothermal actuation allows for the continuous reconfiguration across the entire tunable range, unlike the earlier reported electrostatic approach, which only provides limited accessible range owing to the inherent pull-in phenomenon.[49,50] Additionally, thermal actuation minimizes the stiction issue and ensures repeatable operation of the metadevice.[33,51] The repeatability of our fabricated metadevice is shown in Figure 2e, where the resonance frequency of the metamaterial returns to the initial state of 0.85 THz within 600 s after switching off the device from 550 mA. This recovery of the metamaterial was also confirmed using the digital holographic microscope (see Figure S1b, Supporting Information). The microcantilever goes back to almost 90% of its initial value within 120 s, and it takes ≈600 s to completely get back to its initial state.

To achieve ultrafast resonance modulation at each of the resonance frequency defined by the electrothermally controlled microcantilevers, photoexcitation with 400 nm laser pulses was adopted. Femtosecond laser based optical control provides the most efficient means of achieving ultrafast resonance modulation with sub-nanosecond timescale operation. Here, we exploit the semiconducting nature of the Si substrate that hosts the frequency-agile microcantilever metamaterial to achieve resonance modulation through photoexcitation. However, the charge carrier relaxation time for single crystal Si substrate is typically in µs and hence is not an attractive material choice for ultrafast terahertz modulators.[52,53] To overcome this limitation and to achieve switching speeds in picoseconds, we adopted He^+ ion irradiation technique to induce defect sites in single crystal Si substrate. Based on the density of defects, the charge carrier dynamics and the photoconductivity of Si can be significantly altered.[7,54] By increasing defect density in Si, the life time of photoexcited carriers can be tailored by more than four orders. (See Figure S6, Supporting Information). However, with increased defect states, the photoconductivity reduces and hence the power required for resonance modulation increases, accordingly. Hence, a trade-off must be made with respect to switching speed and switching power. In our experiment, we used 500 keV He^+ ions to irradiate Si substrate with a dose of 5×10^{13} cm^{-2} over a large area of 1.4×1.4 cm^2. The stopping and range of ion in matter (SRIM) simulations show that the end-of-range (EOR) for the chosen irradiation condition in Si is ≈2 µm (see Figure S4, Supporting Information).[55–57] This means that only the charge carriers generated in the top ≈2 µm of Si will show ultrafast relaxation, while the remaining bulk Si still possess slower relaxation. Hence, using conventional 800 nm as optical pump shows a slower relaxation time (see Figure S5a, Supporting Information), as the optical penetration depth is ≈7 µm, which is significantly higher than the EOR value of 2 µm. Hence, we chose 400 nm pump, which has a penetration depth of 0.2 µm, which is significantly lower than EOR value of ≈2 µm (see Figure S5b, Supporting Information).[58]

To experimentally measure the ultrafast modulation of terahertz resonance under optical stimulus, the fabricated metamaterial was characterized in an optical-pump terahertz-probe setup (See Experimental Section). The resonance modulation of the metamaterial with varying pump fluences at input current of 0 mA is shown in **Figure 3**a. With increasing pump fluence, a reduction in the resonance strength and an increase in spectral linewidth is observed. This is caused due to the increase in the conductivity of Si due to photoexcitation. The generated free carriers screen the confined resonant fields, thereby leading to the observed resonance broadening and strength reduction. At the pump fluence of 390 µJ cm^{-2}, complete modulation of dipole resonance at 0.85 THz is achieved. The effect of increasing photoconductivity of Si due to optical pumping on microcantilever metamaterial resonance was simulated. The simulated transmission spectra of the microcantilever metamaterial

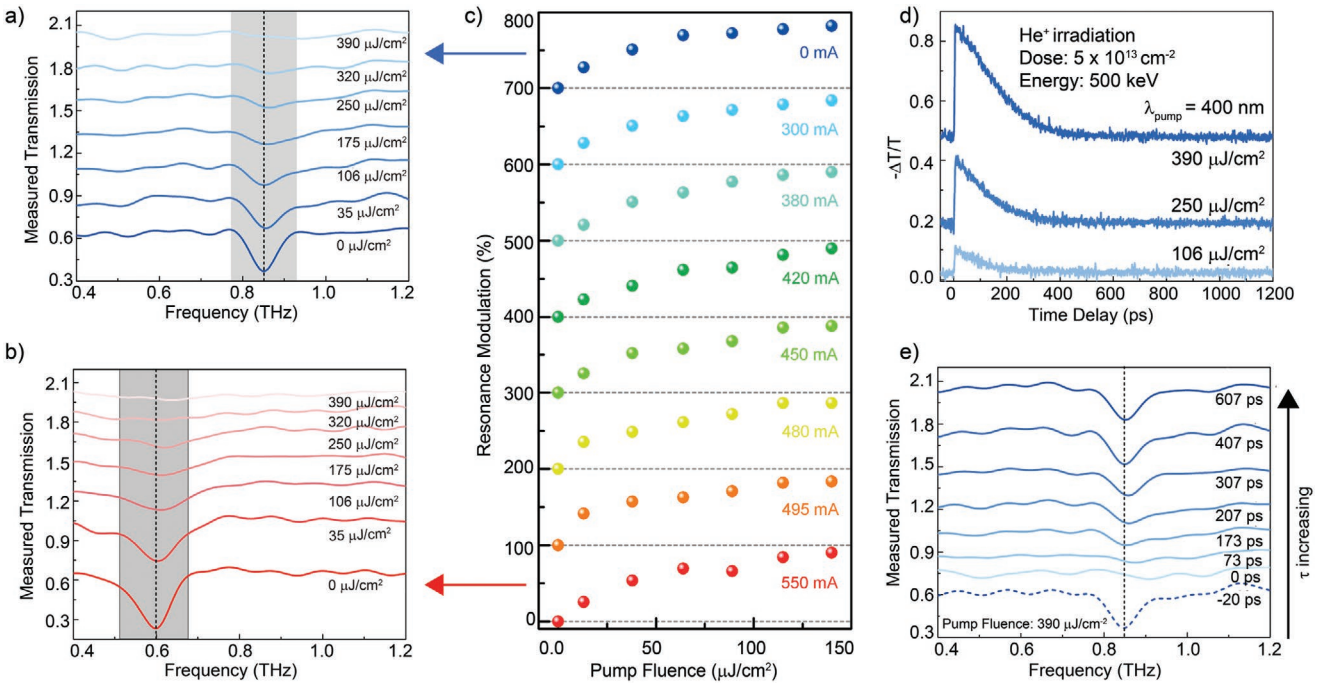

Figure 3. Measured terahertz transmission spectra of the microcantilever metamaterial with varying pump fluence with a) input current = 0 mA and b) input current = 550 mA, respectively. The graphs are vertically offset for clarity. c) Measured resonance modulation of the microcantilever metamaterial with increasing pump fluence and varying input current. d) Measured charge carrier dynamics of optically pumped (λ_{pump} = 400 nm) ion-irradiated Si substrate of the microcantilever metamaterial at varying pump fluence. The maximum $|\Delta T/T|$ value increases with increasing pump fluence. The relaxation time of the photoexcited charge carriers is approximately 400 ps. e) Ultrafast resonance recovery observed from measured terahertz transmission response of microcantilever metamaterial with varying pump-probe delay time ($\Delta\tau$) for pump fluence of 390 μJ cm^{-2}. The dipole resonance is completely modulated at time matched condition ($\Delta\tau$ = 0 ps), when $|\Delta T/T|$ is maximum and starts to recover with increasing $\Delta\tau$. The dipole resonance is completely recovered at 400 ps.

at varying conductivity of 0.2 μm surface of Si substrate is shown in Figure S7, Supporting Information and agrees well with the experimental results. Figure 3b shows the resonance modulation at 0.6 THz by reconfiguring the metamaterial with 550 mA current under varying pump fluences. A similar trend of resonance strength reduction and linewidth broadening was observed with increasing pump fluence. To further demonstrate the ultrafast modulation of terahertz resonance with continuous frequency agility, the resonance frequency was varied by changing the input current and then optical pump fluence was increased to achieve resonance modulation at each of the resonance frequencies. The resonance modulation was calculated as $|T_{OFF} - T_{ON}|/T_{OFF} \times 100\%$, where T_{OFF} and T_{ON} are the resonance strength when the optical pump is OFF and ON, respectively. The resonance strength is defined as the peak to peak transmission value across the resonance.[31] The optically controlled terahertz transmission of the microcantilever metamaterial was measured at different input current values (see Figure S8, Supporting Information) and their corresponding resonance modulation is shown in Figure 3c. At each of the preset resonance frequency, 100% modulation of resonance was achieved. It is also important to elucidate the dependence of resonance modulation through screening effect of photocarriers on the Si surface on the microcantilever position with respect to the Si surface (δ). For 400 nm optical pump, the photocarriers are generated in the top ≈0.2 μm of the Si surface, while the confined terahertz field decays exponentially from the metamaterial resonators in both the out-of-plane directions. Hence, the position of the microcantilever will strongly influence the interaction strength between the confined terahertz field and optically generated free carriers. For the case, when the cantilever is on top of the Si substrate (δ = 0 μm), strong terahertz field confinement overlaps with the photocarrier generated region and hence will lead to a strong modulation of resonance amplitude. However, when the microcantilevers are suspended over the Si substrate, the interacting terahertz field with the photocarriers is much weaker. This understanding is clearly observed from the change in resonance strength at a given photoconductivity (σ_p) of Si surface with varying θ. For any given σ_p, the change in resonance strength is much stronger for θ = 0° and decreases with increase in θ value (see Figure S9a, Supporting Information). The change in resonance strength is calculated for measured spectra at varying pump fluences for input current of 0 and 550 mA further validates the results from the simulation (see Figure S9b, Supporting Information).

The ultrafast behavior of the microcantilever metamaterial was characterized by measuring the charge carrier relaxation dynamics of the metamaterial with varying time delay ($\Delta\tau = \tau_{probe} - \tau_{pump}$) between the optical pump (τ_{pump}) and terahertz probe (τ_{probe}) arrival times, as shown in Figure 3d. Excitation of charge carriers occurs within few picoseconds, while the relaxation takes over hundreds of picoseconds. The sub-ns recovery of photoexcited charge carrier in Si is achieved through defect engineering of single crystal Si using

ion-irradiation technique as mentioned earlier. Figure 3d also shows that with increasing pump fluence, the maximum $|\Delta T/T|$ value increases, leading to a corresponding increase in the photoconductivity of Si (see Figure S6, Supporting Information). This increase in photoconductivity results in the modulation of terahertz resonances with increasing pump fluences as shown in Figure 3c. Furthermore, the switch-off time from the relaxation part of the dynamics is measured to be ≈400 ps. Switch-off time is defined as the time, when the value of $|\Delta T/T|$ comes back to the initial state when there is no pump. In order to validate the ultrafast recovery of terahertz resonance, the transmission characteristics of the metadevice is measured by varying the time delay of the optical pump and the terahertz probe ($\Delta\tau$) for the pump fluence of 390 μJ cm^{-2}. The measured spectra are shown in Figure 3e. At $\Delta\tau = 0$ ps, the pump and probe are time matched and hence a complete modulation of terahertz resonance, due to photoexcitation of Si is observed. With increasing $\Delta\tau$, the number of free carriers decreases and leads to a gradual recovery of terahertz resonance. At $\Delta\tau$ = 400 ps, complete recovery of the terahertz resonance is observed. It is important to note that the overall modulation speed of the microcantilever metamaterial is limited by the switch-off time. The switch-off time can be further improved by increasing the defect density in Si, which can be achieved either through increasing the dose of He^+ ions or by using heavier ions.[54,55] The proposed approach not only provides a means of engineering the temporal response over four orders of magnitude but also alleviates the need for exotic materials to achieve ultrafast modulators. The proposed scheme can be readily expanded to further enable spatial as well as polarization control.[59,60] Complete control of terahertz waves across the varied dimensionality of space, frequency, time, and polarization can be readily realized, which could lead to novel physical phenomenon beyond conventional Lorentzian formalism of electromagnetism.

In conclusion, we have experimentally demonstrated independent manipulation of spectral and temporal response of terahertz waves, through integration of electromechanically reconfigurable microcantilever metamaterial on photoresponsive ion-irradiated Si substrate. Electromechanically reconfigurable microcantilevers enabled a large resonance frequency tunability of 0.25 THz, while optical pumping of ion-irradiated Si substrate hosting the microcantilever metamaterial provided 100% resonance modulation with recovery time of 400 ps. Our proposed approach of integrating complementing technologies of MEMS, optical control using femtosecond laser pulses and ion-irradiated semiconductor provides a unique platform that combines the advantages of individual approaches for multidimensional control of terahertz waves. Hence, it will aid in the development of advanced terahertz components such as spatiotemporal modulators, variable frequency converters and time varying metamaterials for next-generation high-speed terahertz wireless communication channels.

Experimental Section

Sample Preparation: The lightly *p*-doped Si wafer was cleaned and 100 nm thick silicon-di-oxide (SiO_2) layer was deposited using low-pressure chemical vapor deposition (LPCVD). This SiO_2 layer acted as the sacrificial layer to release the bimaterial microcantilevers from the Si substrate. Photolithography was used to define the anchor regions and SiO_2 was selectively dry etched to expose Si substrate. Then, 50 nm thick Al_2O_3 layer was deposited using atomic layer deposition (ALD) process, followed by 300 nm of sputter deposited Al. At this point, the bimorph (Al/Al_2O_3) layers were in physical contact with Si at the anchor region, where the SiO_2 was etched away. While, on the other parts, the bimaterial layer is on top of SiO_2. Second photolithography step was used to define the metamaterial unit cell geometry, metal line, and bond pads, simultaneously. Both Al and Al_2O_3 were dry etched subsequently, this ensured no alignment mismatch of the bimaterial layers forming the microcantilevers. Now, the part of metamaterial unit cells that needed to be released was on top of SiO_2 layer, while the other regions were anchored to Si substrate. Finally, vapor hydrofluoric acid (VHF) was used to isotropically remove the SiO_2 sacrificial layer, thereby suspending the microcantilevers over the Si substrate with an air gap between them. Due to the residual stress in the bimaterial layers, the released cantilevers were bent up, thereby increasing the initial tip displacement (δ). After the release step, the fabricated microcantilever metamaterial was ion-irradiated using He^+ ions of desired energy and dosage. The fabricated metamaterial was then pasted onto a printed circuit board (PCB) with a hole in middle, to allow terahertz transmission measurements. Wire bonding was carried out to connect the metamaterial bond pads to the PCB bond pads. Finally, wires were soldered from the PCB bond pads to enable current control.

Time Resolved Terahertz Time Domain Spectroscopy: The time resolved THz-TDS measurements were carried out using Optical-pump-Terahertz-probe setup that was based on ZnTe nonlinear terahertz generation and detection. Initially the optical beam (800 nm) having pulse energy of 6 mJ pulse^{-1} with pulse width of ≈35 fs and 1 kHz repetition rate was divided into two parts (70:30), where the 70% beam was used for optical pumping of the sample. Further, the 30% beam divided into two parts as (90:10) among them 90% beam was used to generate terahertz by pumping the ZnTe crystal while the other beam was used in electro-optical detection. The photoexcitation pulse of photon energy of 3.1 eV is achieved through second harmonic generation of 1.55 eV incident laser pulse using a BBO crystal. The optical pump beam had a beam diameter of approximately 6 mm, which was larger than the focused terahertz beam diameter of nearly 3 mm at the sample position, providing uniform photoexcitation over the sample. The time delay ($\Delta\tau$) between optical-pump and terahertz probe pulses was controlled by using a translational stage and the pump time delay for the terahertz modulation measurement was set at the position where the photoexcited signal was the maximum ($\Delta\tau \approx 0$ ps). At this maximum pump signal, the terahertz scan was performed for the sample and reference substrate. The electric field of the terahertz waves was polarized parallel to the microcantilever length and illuminated the sample surface at normal incidence. Later, in the post processing steps the transmission spectrum was obtained by taking the ratio of the sample spectra ($E_S(\omega)$) and the reference substrate ($E_R(\omega)$) spectra using the relation $|T(\omega)| = |E_S(\omega)|/|E_R(\omega)|$.

Supporting Information

Supporting Information is available from the Wiley Online Library or from the author.

Acknowledgements

The authors acknowledge the research funding support from National Research Foundation (NRF) Singapore and Agence Nationale de la Recherche (ANR), France- NRF2016- ANR004 (M4197003), NRF CRP on Oxide Electronics on silicon Beyond Moore (NRF-CRP15-2015-01), and Advanced Manufacturing and Engineering (AME) Programmatic grant (A18A5b0056) from Agency for Science, Technology and Research (A*STAR).

Conflict of Interest

The authors declare no conflict of interest.

Author Contributions

P.P. and R.S. conceived and designed research. P.P., S.P., and N.W. fabricated the samples. L.H. under the supervision of A.A.B. carried out the ion irradiation process. P.P. and S.P. performed the electromechanical characterization of the microcantilevers. P.P. and A.K. performed the terahertz characterization of the samples. P.P. wrote the manuscript with support from all authors. R.S., T.V., A.A.B., and C.L. supervised the project.

Keywords

microelectromechanical systems, multifunctional, spatiotemporal metamaterials, ultrafast, terahertz

Received: January 16, 2020
Revised: March 11, 2020
Published online: April 8, 2020

[1] P. H. Siegel, *IEEE Trans. Microwave Theory Tech.* **2002**, *50*, 910.
[2] P. H. Siegel, *IEEE Trans. Microwave Theory Tech.* **2004**, *52*, 2438.
[3] M. Tonouchi, *Nat. Photonics* **2007**, *1*, 97.
[4] H. Liu, H. Zhong, N. Karpowicz, Y. Chen, X. Zhang, *Proc. IEEE* **2007**, *95*, 1514.
[5] H. Song, T. Nagatsuma, *IEEE Trans. Terahertz Sci. Technol.* **2011**, *1*, 256.
[6] K. Sengupta, T. Nagatsuma, D. M. Mittleman, *Nat. Electron.* **2018**, *1*, 622.
[7] R. Ulbricht, E. Hendry, J. Shan, T. F. Heinz, M. Bonn, *Rev. Mod. Phys.* **2011**, *83*, 543.
[8] P. Forn-Díaz, L. Lamata, E. Rico, J. Kono, E. Solano, *Rev. Mod. Phys.* **2019**, *91*, 025005.
[9] T. J. Yen, W. J. Padilla, N. Fang, D. C. Vier, D. R. Smith, J. B. Pendry, D. N. Basov, X. Zhang, *Science* **2004**, *303*, 1494.
[10] H. Tao, N. I. Landy, C. M. Bingham, X. Zhang, R. D. Averitt, W. J. Padilla, *Opt. Express* **2008**, *16*, 7181.
[11] H.-T. Chen, J. F. O'Hara, A. K. Azad, A. J. Taylor, *Laser Photonics Rev.* **2011**, *5*, 513.
[12] N. K. Grady, J. E. Heyes, D. R. Chowdhury, Y. Zeng, M. T. Reiten, A. K. Azad, A. J. Taylor, D. A. R. Dalvit, H.-T. Chen, *Science* **2013**, *340*, 1304.
[13] K. Fan, W. J. Padilla, *Mater. Today* **2015**, *18*, 39.
[14] A. Q. Liu, W. M. Zhu, D. P. Tsai, N. I. Zheludev, *J. Opt.* **2012**, *14*, 114009.
[15] Q. He, S. Sun, L. Zhou, *Research* **2019**, *2019*, 16.
[16] W. J. Padilla, A. J. Taylor, C. Highstrete, M. Lee, R. D. Averitt, *Phys. Rev. Lett.* **2006**, *96*, 107401.
[17] H.-T. Chen, W. J. Padilla, J. M. O. Zide, A. C. Gossard, A. J. Taylor, R. D. Averitt, *Nature* **2006**, *444*, 597.
[18] R. Degl'Innocenti, S. J. Kindness, H. E. Beere, D. A. Ritchie, *Nanophotonics* **2018**, *7*, 127.
[19] H.-T. Chen, J. F. O'Hara, A. K. Azad, A. J. Taylor, R. D. Averitt, D. B. Shrekenhamer, W. J. Padilla, *Nat. Photonics* **2008**, *2*, 295.
[20] P. Pitchappa, M. Manjappa, C. P. Ho, R. Singh, N. Singh, C. Lee, *Adv. Opt. Mater.* **2016**, *4*, 541.
[21] P. Pitchappa, M. Manjappa, C. P. Ho, R. Singh, N. Singh, C. Lee, *Appl. Phys. Lett.* **2016**, *109*, 211103.
[22] A. Chanana, X. Liu, C. Zhang, Z. V. Vardeny, A. Nahata, *Sci. Adv.* **2018**, *4*, eaar7353.
[23] Y. Hu, T. Jiang, J. Zhou, H. Hao, H. Sun, H. Ouyang, M. Tong, Y. Tang, H. Li, J. You, X. Zheng, Z. Xu, X. Cheng, *Adv. Opt. Mater.* **2019**, *7*, 1901050.
[24] S. Zhang, J. Zhou, Y.-S. Park, J. Rho, R. Singh, S. Nam, A. K. Azad, H.-T. Chen, X. Yin, A. J. Taylor, X. Zhang, *Nat. Commun.* **2012**, *3*, 942.
[25] L. Cong, P. Pitchappa, C. Lee, R. Singh, *Adv. Mater.* **2017**, *29*, 1700733.
[26] L. Cong, P. Pitchappa, Y. Wu, L. Ke, C. Lee, N. Singh, H. Yang, R. Singh, *Adv. Opt. Mater.* **2017**, *5*, 1600716.
[27] H.-T. Chen, W. J. Padilla, M. J. Cich, A. K. Azad, R. D. Averitt, A. J. Taylor, *Nat. Photonics* **2009**, *3*, 148.
[28] D. Wang, L. Zhang, Y. Gu, M. Q. Mehmood, Y. Gong, A. Srivastava, L. Jian, T. Venkatesan, C.-W. Qiu, M. Hong, *Sci. Rep.* **2015**, *5*, 15020.
[29] K. Lee, J. Son, J. Park, B. Kang, W. Jeon, F. Rotermund, B. Min, *Nat. Photonics* **2018**, *12*, 765.
[30] Z. T. Ma, Z. X. Geng, Z. Y. Fan, J. Liu, H. D. Chen, *Research* **2019**, *2019*, 6482975.
[31] W. X. Lim, M. Manjappa, Y. K. Srivastava, L. Cong, A. Kumar, K. F. MacDonald, R. Singh, *Adv. Mater.* **2018**, *30*, 1705331.
[32] D. R. Chowdhury, R. Singh, A. J. Taylor, H.-T. Chen, A. K. Azad, *Appl. Phys. Lett.* **2013**, *102*, 011122.
[33] P. Pitchappa, M. Manjappa, H. N. S. Krishnamoorthy, Y. Chang, C. Lee, R. Singh, *Appl. Phys. Lett.* **2017**, *111*, 261101.
[34] A. Chanana, Y. Zhai, S. Baniya, C. Zhang, Z. V. Vardeny, A. Nahata, *Nat. Commun.* **2017**, *8*, 1328.
[35] M. Manjappa, A. Solanki, A. Kumar, T. C. Sum, R. Singh, *Adv. Mater.* **2019**, *31*, 1901455.
[36] Y. K. Srivastava, A. Chaturvedi, M. Manjappa, A. Kumar, G. Dayal, C. Kloc, R. Singh, *Adv. Opt. Mater.* **2017**, *5*, 1700762.
[37] S. Arezoomandan, P. Gopalan, K. Tian, A. Chanana, A. Nahata, A. Tiwari, B. Sensale-Rodriguez, *IEEE J. Sel. Top. Quantum Electron.* **2017**, *23*, 188.
[38] J. Shi, Z. Li, D. K. Sang, Y. Xiang, J. Li, S. Zhang, H. Zhang, *J. Mater. Chem. C* **2018**, *6*, 1291.
[39] Y. Hu, T. Jiang, J. Zhou, H. Hao, H. Sun, H. Ouyang, M. Tong, Y. Tang, H. Li, J. You, X. Zheng, Z. Xu, X. Cheng, *Nano Energy* **2020**, *68*, 104280.
[40] P. Pitchappa, A. Kumar, S. Prakash, H. Jani, T. Venkatesan, R. Singh, *Adv. Mater.* **2019**, *31*, 1808157.
[41] H. Cai, S. Chen, C. Zou, Q. Huang, Y. Liu, X. Hu, Z. Fu, Y. Zhao, H. He, Y. Lu, *Adv. Opt. Mater.* **2018**, *6*, 1800257.
[42] R. Singh, J. Xiong, A. K. Azad, H. Yang, S. A. Trugman, Q. X. Jia, A. J. Taylor, H.-T. Chen, *Nanophotonics* **2012**, *1*, 117.
[43] Y. K. Srivastava, M. Manjappa, L. Cong, H. N. S. Krishnamoorthy, V. Savinov, P. Pitchappa, R. Singh, *Adv. Mater.* **2018**, *30*, 1801257.
[44] S. Chen, Z. Li, W. Liu, H. Cheng, J. Tian, *Adv. Mater.* **2019**, *31*, 1802458.
[45] S. Chen, W. Liu, Z. Li, H. Cheng, J. Tian, *Adv. Mater.* **2020**, *32*, 1805912.
[46] P. Pitchappa, C. P. Ho, L. Dhakar, Y. Qian, N. Singh, C. Lee, *J. Microelectromech. Syst.* **2015**, *24*, 525.
[47] P. Pitchappa, C. P. Ho, Y. Qian, L. Dhakar, N. Singh, C. Lee, *Sci. Rep.* **2015**, *5*, 11678.
[48] D. J. Park, S. J. Park, I. Park, Y. H. Ahn, *Curr. Appl. Phys.* **2014**, *14*, 570.
[49] Z. Han, K. Kohno, H. Fujita, K. Hirakawa, H. Toshiyoshi, *Opt. Express* **2014**, *22*, 21326.
[50] M. Unlu, M. Jarrahi, *Opt. Express* **2014**, *22*, 32245.
[51] C. P. Ho, P. Pitchappa, Y.-S. Lin, C.-Y. Huang, P. Kropelnicki, C. Lee, *Appl. Phys. Lett.* **2014**, *104*, 161104.
[52] J. Gu, R. Singh, X. Liu, X. Zhang, Y. Ma, S. Zhang, S. A. Maier, Z. Tian, A. K. Azad, H.-T. Chen, A. J. Taylor, J. Han, W. Zhang, *Nat. Commun.* **2012**, *3*, 1151.

[53] M. Manjappa, Y. K. Srivastava, L. Cong, I. Al-Naib, R. Singh, *Adv. Mater.* **2017**, *29*, 1603355.
[54] F. E. Doany, D. Grischkowsky, C. C. Chi, *Appl. Phys. Lett.* **1987**, *50*, 460.
[55] J. P. Biersack, J. F. Ziegler, in *Ion Implantation Techniques*, (Eds: H. Ryssel, H. Glawischnig), Springer Series in Electrophysics, vol. *10*, Springer, Berlin **1982**.
[56] S. Azimi, J. Song, Z. Y. Dang, H. D. Liang, M. B. H. Breese, *J. Micromech. Microeng.* **2012**, *22*, 113001.
[57] H. D. Liang, S. K. Vanga, J. F. Wu, B. Q. Xiong, C. Y. Yang, A. A. Bettiol, M. B. H. Breese, *Opt. Express* **2015**, *23*, 121.
[58] A. Kumar, Y. K. Srivastava, M. Manjappa, R. Singh, *Adv. Opt. Mater.* **2018**, *6*, 1800030.
[59] P. Pitchappa, C. P. Ho, L. Dhakar, C. Lee, *Optica* **2015**, *2*, 571.
[60] P. Pitchappa, C. P. Ho, L. Cong, R. Singh, N. Singh, C. Lee, *Adv. Opt. Mater.* **2016**, *4*, 391.